

Binuclear Rhodium Hydride Complexes: Synthesis, Structure, and Reactivity

Faisal Shafiq and Richard Eisenberg*

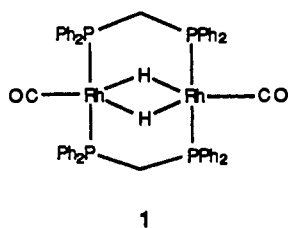
Department of Chemistry, University of Rochester, Rochester, New York 14627

Received December 23, 1992

The formation of binuclear rhodium hydride complexes has been accomplished by reaction of the corresponding chloro complexes with the hydride reducing agents NaBH_4 and LiAlH_4 . For the A-frame complex $\text{Rh}_2\text{Cl}_2(\mu\text{-CO})(\text{dppm})_2$ (dppm = bis(diphenylphosphino)-methane), reaction with NaBH_4 in toluene/MeOH leads to the borohydride-coordinated complex $\text{Rh}_2(\text{BH}_4)_2(\mu\text{-CO})(\text{dppm})_2$, **2**, whereas, in THF/MeOH, the same reactants yield the tetrahydride species $\text{Rh}_2(\mu\text{-H})_2\text{H}_2(\text{CO})(\text{dppm})_2$, **3**. Reduction of $\text{Rh}_2\text{Cl}_2(\mu\text{-CO})(\text{dppm})_2$ with LiAlH_4 in THF leads to the formation of $\text{Rh}_2(\text{AlH}_4)_2(\mu\text{-CO})(\text{dppm})_2$, **4**, which is only obtained *in situ*. Complexes **2–4** have been characterized by ^1H , ^{31}P , and ^{13}C NMR and IR spectroscopies. Complex **3** loses H_2 reversibly, accompanied by a color change from orange under H_2 to olive green under vacuum. For the 2-(diphenylphosphino)pyridine-bridged complex $\text{Rh}_2(\mu\text{-CO})\text{Cl}_2(\text{Ph}_2\text{Ppy})_2$, reaction with NaBH_4 leads to the formation of the borohydride complex $\text{Rh}_2(\mu\text{-CO})(\text{BH}_4)_2(\text{Ph}_2\text{Ppy})_2$, **5**, which is characterized by a single-crystal X-ray diffraction study as well as by ^1H and ^{31}P NMR and IR spectroscopies. The crystals of **5** are triclinic (space group $P\bar{1}$) having a unit cell of dimensions $a = 10.680(4)$ Å, $b = 15.954(4)$ Å, $c = 23.018(5)$ Å, $\alpha = 89.09(2)^\circ$, $\beta = 84.20(2)^\circ$, $\gamma = 77.28(3)^\circ$, $V = 3806.3$ Å³, and $Z = 4$, with two pairs of independent binuclear complexes per unit cell. Complex **5** possesses a distorted A-frame structure in which the Rh centers are bridged by two Ph_2Ppy ligands in a head to tail fashion, with CO occupying the bridgehead position. On the basis of spectroscopic evidence, the BH_4^- ligand is assigned an η^2 mode of coordination to the Rh center. The Rh–Rh bond distance is 2.645(5) Å. From spectroscopic data, the bis(tetrahydridoaluminate) complex **4** appears to have the same structure as **2**. The reactivity of compounds **2–5** with CO, olefins, and D_2 have been examined. Complexes **2**, **4**, and **5** catalyze ethylene hydrogenation rather slowly; however, the tetrahydride complex **3** is quite active.

Introduction

Binuclear rhodium hydrides bridged by the bis(phosphine) ligand 1,1-bis(diphenylphosphino)methane or dppm have served as models for rhodium-based hydrogenation catalyst systems. A number of geometries including A-frames, cradle, and mixed structures have been identified with these dppm -bridged binuclear systems.^{1–12} One specific complex of interest that has been the subject of study in our laboratory is the dihydride $\text{Rh}_2\text{H}_2(\text{CO})_2(\text{dppm})_2$, **1**, synthesized by the NaBH_4 reduction of



1

$\text{Rh}_2\text{Cl}_2(\text{CO})_2(\text{dppm})_2$.⁹ This complex was observed to be highly reactive with acetylenes, leading to the formation of vinylidene

complexes, and served as an entry point to the synthesis of A-frame and other binuclear complexes. Complex **1** was also found to catalyze hydrogenation reactions and, in the presence of H_2 enriched in the para spin state, led to enhanced resonances in product ^1H NMR spectra due to parahydrogen-induced polarization. The iridium dihydride system analogous to **1** as well as Rh–Ir heterobimetallic hydride complexes have been described in the last several years by Cowie and co-workers.^{3,11,13–17}

In this paper we describe the hydride reductions of the binuclear monocarbonyl complexes $\text{Rh}_2\text{Cl}_2(\mu\text{-CO})(\text{dppm})_2$ and $\text{Rh}_2\text{Cl}_2(\mu\text{-CO})(\text{Ph}_2\text{Ppy})_2$. The dppm -bridged chloro complex $\text{Rh}_2\text{Cl}_2(\mu\text{-CO})(\text{dppm})_2$ was first reported by Cowie and co-workers and possesses an A-frame structure.¹⁸ The Ph_2Ppy -bridged species was initially synthesized by Balch *et al.* and has a distorted A-frame structure as a consequence of the smaller bite of the Ph_2Ppy bridge relative to that of dppm .¹⁹ In their studies, Balch *et al.* found that the phosphinopyridyl ligand forms bis-bridged structures in generally a head-to-tail manner—*i.e.*, each metal of the binuclear complex is coordinated to one N and one P from the two Ph_2Ppy ligands. The reductions lead to the synthesis, characterization, and reaction chemistry of a tetrahydride binuclear complex of rhodium, bis(borohydride) A-frame complexes, and the observation of an analogous tetrahydridoaluminate species. For the dppm system, the latter two compounds are intermediates en route to the formation of the tetrahydride complex. To date, very few examples of dppm -bridged tetrahy-

- Balch, A. L. In *Homogeneous Catalysis with Metal Phosphine Complexes*; Pignolet, L. H., Ed.; Plenum Press: New York, 1983; p 167.
- Puddephatt, R. *J. Chem. Soc. Rev.* **1983**, *12*, 99.
- Berry, D. H.; Eisenberg, R. *Organometallics* **1987**, *6*, 1796–1805.
- Cowie, M.; Dwight, S. K.; Sanger, A. R. *Inorg. Chim. Acta* **1978**, *31*, L407–L409.
- Cowie, M.; Dickson, R. S. *Inorg. Chem.* **1981**, *20*, 2682–2688.
- Vaartstra, B. A.; O'Brien, K. N.; Eisenberg, R.; Cowie, M. *Inorg. Chem.* **1988**, *27*, 3668–3672.
- Vaartstra, B. A.; Cowie, M. *Inorg. Chem.* **1989**, *28*, 3138–3147.
- Muralidharan, S.; Espenson, J. H. *J. Am. Chem. Soc.* **1984**, *106*, 8104–8109.
- Woodcock, C.; Eisenberg, R. *Inorg. Chem.* **1984**, *23*, 4207–4211.
- Woodcock, C.; Eisenberg, R. *Inorg. Chem.* **1985**, *24*, 1285–1287.
- Kubiak, C. P.; Woodcock, C.; Eisenberg, R. *Inorg. Chem.* **1982**, *21*, 2119–2129.
- Wang, W.-D.; Hommeltoft, S. I.; Eisenberg, R. *Organometallics* **1988**, *7*, 2417–2419.

- Eisenberg, R. *Acc. Chem. Res.* **1991**, *24*, 110–116.
- Eisenschmid, T. C.; Kirss, R. U.; Peutsch, P. P.; Hommeltoft, S. I.; Eisenberg, R.; Bargon, J.; Lawler, R. G.; Balch, A. L. *J. Am. Chem. Soc.* **1987**, *109*, 8089–8091.
- Hommeltoft, S. I.; Berry, D. H.; Eisenberg, R. *J. Am. Chem. Soc.* **1986**, *108*, 5345–5347.
- McDonald, R.; Sutherland, B. R.; Cowie, M. *Inorg. Chem.* **1987**, *26*, 3333–3339.
- McDonald, R.; Cowie, M. *Inorg. Chem.* **1990**, *29*, 1564–1571.
- Cowie, M.; Dwight, S. K. *Inorg. Chem.* **1980**, *19*, 2508–2513.
- Farr, J. P.; Olmstead, M. M.; Balch, A. L. *J. Am. Chem. Soc.* **1980**, *102*, 6654–6656.

dride and borohydride complexes have been isolated. These include the cis and trans isomers of the tetrahydride complex $\text{Ir}_2\text{H}_4(\text{CO})(\text{dppm})_2$ observed in the NaBH_4 reduction of $\text{Ir}_2\text{Cl}_2(\text{CO})_2(\text{dppm})_2$ by Cowie.¹⁶

Experimental Section

Materials, Methods, and Preparations. Rhodium trichloride trihydrate (Johnson-Matthey) and the ligand bis(diphenylphosphino)methane (Strem) or dppm were used as received without further purification. The ligand 2-(diphenylphosphino)pyridine (Ph_2Ppy)^{19,20} and the starting complexes $\text{Rh}_2(\mu\text{-CO})\text{Cl}_2(\text{Ph}_2\text{Ppy})_2$,¹⁹ $\text{Rh}_2\text{Cl}_2(\mu\text{-CO})(\text{dppm})_2$, and $\text{Rh}_2(\text{CH}_3)_2(\mu\text{-CO})(\text{dppm})_2$ were prepared according to published procedures from $\text{Rh}_2\text{Cl}_2(\text{CO})_2(\text{dppm})_2$.^{18,21,22} All syntheses were performed under N_2 using standard Schlenk and inert-atmosphere techniques. All solvents used were of reagent grade and were dried and degassed before use. THF and C_6H_6 were dried using Na-benzophenone ketyl and were vacuum distilled. CH_3OH and CH_3CN were dried with CaH_2 prior to vacuum distillation. Infrared spectra were obtained on a Mattson 6020 Galaxy series FTIR spectrometer. ^1H and ^{31}P NMR spectra were recorded on a Bruker AMX-400 spectrometer at field strengths of 400.13 and 161.92 MHz, respectively. Chemical shifts for ^1H NMR spectra are reported in ppm downfield from tetramethylsilane but were measured relative to residual ^1H resonances in the deuterated solvents (C_6D_6 , δ 7.15 ppm, and THF- d_7 , δ 3.65 ppm). ^{31}P chemical shifts are reported in ppm downfield from phosphoric acid and were referenced to external 85% H_3PO_4 . The X-ray structure determination of complex 5 was performed on an Enraf-Nonius CAD4 diffractometer at -20°C .

$[\text{Rh}_2(\text{BH}_4)_2(\mu\text{-CO})(\text{dppm})_2]$ (2). In a 50-mL round-bottom flask are placed 0.100 g (93 μmol) of $\text{Rh}_2\text{Cl}_2(\mu\text{-CO})(\text{dppm})_2$ and 0.100 g (2.6 mmol) of NaBH_4 under a H_2 purge. A solvent mixture of 6 mL of dry MeOH /toluene (1:1 v/v ratio) is injected into the flask. Vigorous gas evolution is observed as NaBH_4 reacts with $\text{Rh}_2\text{Cl}_2(\mu\text{-CO})(\text{dppm})_2$. After 30 min, the reaction is complete and an air-stable yellow precipitate has formed. CH_3CN may also be used as the solvent in this synthesis. The precipitate is filtered out in air and isolated in 89% yield.

Spectroscopic Data. ^1H NMR (C_6D_6): δ 3.10 ppm (mult 2 H; dppm $-\text{CH}_2-$), 3.63 ppm (mult 2 H; dppm $-\text{CH}_2-$), -1.49 ppm (broad; 8 H; BH_4^-), 6.75–7.74 ppm (40 H; dppm phenyl). $^{31}\text{P}\{^1\text{H}\}$ NMR (C_6D_6): δ 23.97 ppm (AA'A''A'''XX' pattern; $J_{\text{Rh-P}} = 131$ Hz). $^{13}\text{C}\{^1\text{H}\}$ NMR (CH_2Cl_2): δ 243.6 ppm (t of q; $J_{\text{Rh-C}} = 42$ Hz; $J_{\text{C-P}} = 8$ Hz; $\mu\text{-CO}$). IR (CH_2Cl_2): 1738 cm^{-1} (ν_{CO} = 1698 cm^{-1}); 2422, 2384 cm^{-1} (terminal B–H stretch); 1364 cm^{-1} (bridge stretch); 1145 cm^{-1} (BH_2 deformation).

$[\text{Rh}_2(\mu\text{-CO})(\text{BD}_4)_2(\text{dppm})_2]$ (2-d₈). NaBD_4 is used in place of NaBH_4 in the synthesis of complex 2-d₈. The synthesis is otherwise completely analogous to that of complex 2.

$[\text{Rh}_2(\mu\text{-H})_2\text{H}_2(\text{CO})(\text{dppm})_2]$ (3). **Method A.** In a 50-mL round-bottom flask, 0.150 g (145 μmol) of complex 2 is dissolved in 1.5 mL of a 3:1 (v/v) mixture of THF/ MeOH . Gas evolution is observed as an orange/red solution of $\text{Rh}_2(\mu\text{-H})_2\text{H}_2(\text{CO})(\text{dppm})_2$, 3, forms after 30 min at room temperature. Addition of 5 mL of olefin-free hexanes precipitates 3 as an orange solid, which is then filtered in the drybox and isolated in 79% yield.

Spectroscopic Data. ^1H NMR (THF- d_8): δ 4.04 ppm (broad s; 4 H; dppm $-\text{CH}_2-$); 7.02–7.77 ppm (40 H; dppm phenyl); -9.24 ppm (broad; 2 H; bridging Rh–H); -10.45 ppm (broad; 2 H; terminal Rh–H). $^{31}\text{P}\{^1\text{H}\}$ NMR δ 37.8 ppm (XX'YY'AB pattern); 47.4 ppm (XX'YY'AB pattern). IR (KBr): $\nu_{\text{CO}} = 1965$ cm^{-1} ; $\nu_{\text{H-CO}} = 1878$ cm^{-1} ; 3:1 (v:v) THF/ MeOH , $\nu_{\text{CO}} = 1932$ cm^{-1} . Anal. Calcd for $\text{C}_{51}\text{H}_{48}\text{OP}_4\text{Rh}_2$: C, 60.85; H, 4.81. Found: C, 59.53; H, 4.88.

Method B. In a 50-mL round bottom flask are placed 0.040 g (37 μmol) of $\text{Rh}_2\text{Cl}_2(\mu\text{-CO})(\text{dppm})_2$ and 0.015 g NaBH_4 under a stream of H_2 . Upon addition of 3 mL of a 3:1 (v/v) mixture of THF/ MeOH saturated with H_2 , vigorous gas evolution is observed as $\text{Rh}_2\text{Cl}_2(\mu\text{-CO})(\text{dppm})_2$ dissolves to form an orange/red solution of complex 3. After 1 h, 10 mL of dry ethanol is added to precipitate complex 3 as an orange solid. The orange solid can be filtered out in air and isolated in 70% yield. The solid is then stored under either N_2 or H_2 (1 atm).

Method C. In an NMR tube, 0.010 g (9.7 μmol) of the previously characterized complex $\text{Rh}_2(\text{CH}_3)_2(\mu\text{-CO})(\text{dppm})_2$ is dissolved in C_6D_6 .

The sample is then placed under 1 atm of H_2 . Quantitative conversion to 3 is observed by ^1H and ^{31}P NMR spectroscopies, as is the evolution of CH_4 .

In Situ Generation of $[\text{Rh}_2(\text{AlH}_4)_2(\mu\text{-CO})(\text{dppm})_2]$ (4). In an NMR tube, 0.010 g (9.3 μmol) of $\text{Rh}_2\text{Cl}_2(\mu\text{-CO})(\text{dppm})_2$ is suspended in THF- d_8 . A 0.004-g amount (106 μmol) of LiAlH_4 is then added to the sample under N_2 , and the system is allowed to react at room temperature. Gas evolution is immediate as $\text{Rh}_2\text{Cl}_2(\mu\text{-CO})(\text{dppm})_2$ reacts with LiAlH_4 to form an orange solution of complex 4 within 15 min. Complex 4 is not isolable even at -30°C as it reacts with MeOH , EtOH , CH_3CN , H_2O , and Et_2O used to remove excess LiAlH_4 . Complex 4 reacts with these common solvents to produce the tetrahydride complex 3.

Spectroscopic Data. ^1H NMR (THF- d_8): δ 3.00 ppm (broad d; $J = 15$ Hz; 2 H; dppm $-\text{CH}_2-$), 3.85 ppm (mult; 2 H; dppm $-\text{CH}_2-$), 2.80 ppm (terminal Al–H), 6.88–7.94 ppm (40 H, dppm phenyl), -5.10 ppm (d; $J = 11$ Hz; 2 H; Al–H), -6.90 ppm (broad; 2 H, Al–H). $^{31}\text{P}\{^1\text{H}\}$ NMR: δ 52.8 ppm ($J_{\text{Rh-P}} = 137.6$ Hz). ^{13}C NMR: δ 271.6 ppm ($J_{\text{Rh-C}} = 32.7$ Hz, $J_{\text{C-P}} = 9$ Hz; $\mu\text{-CO}$). IR (THF): $\nu_{\text{CO}} = 1693$ cm^{-1} .

$\text{Rh}_2(\mu\text{-CO})(\text{BH}_4)_2(\text{Ph}_2\text{Ppy})_2$ (5). In a 50-mL round bottom flask, 0.150 g (0.21 mmol) of $\text{Rh}_2(\mu\text{-CO})\text{Cl}_2(\text{Ph}_2\text{Ppy})_2$ is dissolved in 10 mL of a (v/v) 1:3:1 mixture of THF: CH_2Cl_2 : MeOH . To this suspension is added 0.038 g (1.00 mmol) of NaBH_4 . The reaction is allowed to proceed for 1.5 h under a flow of H_2 . No significant color change is observed. All solvent is removed, and a red solid remained, which was recrystallized from $\text{CH}_2\text{Cl}_2/\text{EtOH}$ at -25°C . Crystals suitable for X-ray analysis are obtained by this procedure. The IR spectrum (CH_2Cl_2) shows ν_{CO} at 1783 cm^{-1} . ^1H NMR (C_6D_6): δ -0.09 (broad, 8H), 6.22 (t, 2H), 6.43 (t, 2H), 6.51 (d, 2H), 6.9–7.8 (20H), 9.11 (d, 2H). ^{31}P NMR (C_6D_6): δ +44.45. Anal. Calcd: C, 53.21; H, 4.60. Found: C, 53.50; H, 4.63.

Preparation of $\text{Rh}_2(\mu\text{-CO})(\text{BD}_4)_2(\text{Ph}_2\text{Ppy})_2$ (5-d₈). Complex 5-d₈ is prepared by the same procedure as complex 5 using >99% NaBD_4 .

Reaction of 2 with D_2 . In an NMR tube, 0.010 g (9.7 μmol) of complex 2 is dissolved in C_6D_6 , and the solution is placed under 1 atm of D_2 . Liberation of H_2 and HD is evidenced within 10 min by the appearance of a singlet at δ 4.45 and a 1:1:1 triplet at δ 4.42 ppm, respectively, in the ^1H NMR spectrum. A 25% decrease in the intensity of the BH_4^- resonance at δ -0.49 ppm is also observed after this time, consistent with deuterium exchange into the BH_4^- unit. After 5 h, a 75% decrease in the intensity of the BH_4^- resonance is observed. Significant catalyst decomposition is also noted within this time period. The decomposition of complex 2 occurs more quickly in other solvents.

Reaction of 2 with Ethylene. In an NMR tube, 0.010 g (9.7 μmol) of 2 is dissolved in CD_2Cl_2 , and the solution is placed under approximately 150 Torr of ethylene and allowed to react at room temperature. Formation of C_2H_6 is observed by ^1H NMR spectroscopy within 5 min as evidenced by the appearance of a singlet at δ 0.85 ppm. Partial decomposition of the metal complex is also seen. After 3 h, some starting material is still observed along with a number of unidentified metal products.

Reaction of 2 with CO. In an NMR tube, 0.010 g (9.7 μmol) of complex 2 is dissolved in C_6D_6 , and the solution is placed under 300 Torr of CO. The reaction proceeds at room temperature to give the known complex $\text{Rh}_2(\text{CO})_3(\text{dppm})_2$, 6, quantitatively within 15 min. Characteristic ^1H and $^{31}\text{P}\{^1\text{H}\}$ NMR resonances for complex 6 at δ 4.43 and 7.15–7.81 ppm and at δ 19.19 ppm, respectively, match those of an authentic sample.¹⁰

Reaction of 2 with THF/ MeOH . In an NMR tube, 0.010 g (9.7 μmol) of 2 is dissolved in a 3:1 (v/v) ratio of THF- d_8 : CD_3OD and the reaction is followed by ^1H NMR spectroscopy at room temperature. H_2 evolution is observed as complex 2 slowly reacts with the solvent mixture to form quantitatively an orange/red solution of complex 3 within 0.5 h.

Reaction of 3 with D_2 . In an NMR tube, 0.015 g (15 μmol) of 3 is dissolved in THF- d_8 , and the solution is then placed under 1 atm of D_2 at room temperature. An 86% decrease in the intensity of the terminal hydride resonance and a 79% decrease in the bridging hydride resonance is observed by ^1H NMR spectroscopy after 15 min. The concurrent observation of a 1:1:1 triplet at δ +4.53 ppm for free HD confirms deuterium exchange between free D_2 and the metal hydrides at room temperature.

Reaction of 3 with CO. In an NMR tube, 0.015 g (15 μmol) of 3 is dissolved in THF- d_8 . The sample is frozen in liquid N_2 and then placed under 400 Torr of CO to prevent reaction at room temperature. The sample is thawed in a dry ice/acetone bath before being placed in an NMR probe precooled to 243 K. Liberation of H_2 and the appearance of complexes 1 and 5 are observed by ^1H and ^{31}P NMR spectroscopies.^{9,10} As the reaction proceeds to completion, only the tricarbonyl complex 6 is observed.

(20) Mann, F. G.; Watson, J. J. *Org. Chem.* 1948, 13, 502–531.

(21) Kramarz, K. W.; Eisenschmid, T. C.; Deutsch, D. A.; Eisenberg, R. J. *Am. Chem. Soc.* 1991, 113, 5090–5092.

(22) Mague, J. T.; Mitchener, J. P. *Inorg. Chem.* 1969, 8, 119–125.

Table I. Summary of Crystallographic Data for $\text{Rh}_2(\text{CO})(\text{BH}_4)_2(\text{Ph}_2\text{Ppy})_2$ (**5**)

empirical formula	$\text{B}_2\text{C}_{35}\text{H}_{36}\text{N}_2\text{O}_2\text{P}_2\text{Rh}_2$
fw	781.99
space group	$P\bar{1}$ (No. 2)
Z	4
a, Å	10.680(4)
b, Å	15.954(4)
c, Å	23.018(5)
α , deg	89.09(3)
β , deg	84.20(2)
γ , deg	77.28(1)
V, Å ³	3806.32
d_{calc} , g/cm ³	1.379
T, °C	-20.0
μ , cm ⁻¹	9.6
$\lambda_{\text{Mo K}\alpha}$ (graphite-monochromated radiation)	0.710 69
agreement of equiv data (F_o)	0.19
R_1^a	0.075
R_2^a	0.083

^a $R_1 = \{\sum||F_o| - |F_c||\} / \{\sum|F_o|\}$; $R_2 = [\sum w(|F_o| - |F_c|)^2]^{1/2} / \{\sum wF_o^2\}$, where $w = [\sigma^2(F_o) + (\rho F_o^2)^2]^{1/2}$ for the non-Poisson contribution weighting scheme. The quantity minimized was $\sum w(|F_o| - |F_c|)^2$. Source of scattering factors f_o , f' , and f'' : Cromer, D. T.; Waber, J. T. *International Tables for X-Ray Crystallography*; Kynoch Press: Birmingham, England, 1974; Vol. IV, Tables 2.2B and 2.3.1.

Reaction of 3 with Olefins/H₂. In an NMR tube, 0.015 g (15 μmol) of **3** is dissolved in C_6D_6 and 3 μL of a standard (THF or dioxane) is injected. A ¹H NMR spectrum is recorded to integrate the amount of complex **3** relative to an internal standard. The sample is frozen, and the particular olefin is then injected into the sample and placed under 3 atm of H₂. The hydrogenation is followed by ¹H NMR spectroscopy at hourly intervals. Turnovers are estimated by integrating resonances of the hydrogenated product relative to the standard present. Complex **3** is not observed during the course of the hydrogenations or after all of the substrate has been hydrogenated.

Reaction of 5 with D₂. In an NMR tube, 0.010 g (13 μmol) of **5** was dissolved in C_6D_6 . Slight deuterium incorporation into the tetrahydridoborate ligand was evidenced by a 6% decrease in the intensity of the BH₄⁻ resonance and the appearance of a 1:1:1 triplet at δ 4.45 ppm in the ¹H NMR spectrum characteristic of free HD after 17 h.

Reaction of 5 with Olefins and H₂. In an NMR tube, 0.010 g (13 μmol) of **5** is dissolved in C_6D_6 and then 4 μL of *tert*-butylethylene (78 μmol) is injected. This solution was then placed under 600 Torr of H₂, and the reaction was followed by ¹H NMR spectroscopy. The formation of 2.3 equiv of the hydrogenated product 2,2-dimethylbutane relative to catalyst concentration was seen after a 48-h period at room temperature. Similarly, in an NMR tube, 0.010 g (13 μmol) of **5** was dissolved in C_6D_6 and placed under 150 Torr of C₂H₄ and 600 Torr of H₂. The formation of at least 1 equiv of ethane relative to catalyst concentration was seen after 5 min by ¹H NMR spectroscopy. In an NMR tube 0.010 g (13 μmol) of **5** was dissolved in C_6D_6 and placed under 400 Torr of CO. No reaction was observed by ¹H NMR spectroscopy even after heating at 60 °C for 24 h.

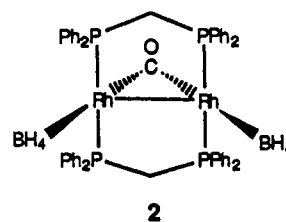
X-ray Structure Determination on Rh₂(μ -CO)(BH₄)₂(Ph₂Ppy)₂, **5.** Red crystals were grown from a saturated CH₂Cl₂ solution at -20 °C. A crystal (0.2 × 0.2 × 0.3 mm) was attached with epoxy to a glass fiber. Crystal data and data collection parameters are summarized in Table I. The initial cell determination was carried out with 25 centered reflections from different parts of reciprocal space with θ between 5 and 13°. The triclinic cell was determined using the Enraf-Nonius CAD4-SDP peak search, centering, and indexing programs and was confirmed with the cell reduction program TRACER. The intensity data for the structure of complex **5** showed no evidence of decay upon X-ray irradiation. The data was only collected to a maximum 2θ of 40° due to weak reflections at higher values. Heavy-atom methods were employed to locate the rhodium atoms, and the DIRDIF program was used for structure expansion. Subsequent cycles of least-squares refinements and difference Fourier maps located the remaining non-hydrogen atoms. After isotropic refinement, an empirical absorption correction (DIFABS) was applied.²³ Assignment of the space group as the centrosymmetric group $P\bar{1}$ is supported by successful refinement of the crystal structure. In the last refinement model, all of the nitrogen and carbon atoms were defined by

(23) Walker, N.; Stuart, D. *Acta Crystallogr.* **1983**, *A39*, 158-166.

isotropic thermal parameters. Hydrogen atoms were placed in calculated positions around the phenyl and pyridyl rings. The supplementary material contains final thermal parameters and complete tabulations of bond distances and angles for the structure.

Results and Discussion

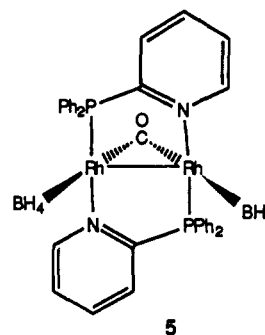
Reduction with NaBH₄. The reaction of $\text{Rh}_2\text{Cl}_2(\mu\text{-CO})(\text{dppm})_2$ with excess NaBH₄ under H₂ in either a MeOH/toluene mixture or in CH₃CN results in the formation of an orange air-stable precipitate which on the basis of the evidence given below is assigned as $\text{Rh}_2(\mu\text{-CO})(\text{BH}_4)_2(\text{dppm})_2$, **2**. The orange solid is



soluble in C₆H₆, toluene, acetone, and CH₂Cl₂. A CD₂Cl₂ solution of this orange solid re-forms the starting dichloride $\text{Rh}_2\text{Cl}_2(\mu\text{-CO})(\text{dppm})_2$ after 4 days at room temperature as observed by ¹H and ³¹P{¹H} NMR spectroscopies. The ¹H NMR (CD₂Cl₂) spectrum of the orange solid exhibits characteristic resonances at δ 3.10 (mult, 2 H), 3.63 (mult, 2 H) ppm and a broad resonance at δ -1.49 (8 H) ppm. The resonances at δ 3.10 and 3.63 ppm are assigned to inequivalent dppm methylene protons. The broad resonance at δ -1.49 ppm is absent in the deuterated complex **2-d₈**, made using NaBD₄, and is therefore assigned to BH₄⁻ ligands bound to the rhodium centers. On the basis of integration, the ratio of dppm: BH₄⁻ ligands in **2** is 1:1. The fact that there is only one broad resonance for the BH₄⁻ ligands suggests that the borohydride hydrogens are undergoing rapid exchange on the NMR time scale.

By ³¹P{¹H} NMR spectroscopy, a single symmetrical second-order pattern is observed at δ 23.97 ppm (AA'A''A'''XX') indicative of four chemically equivalent phosphorus nuclei. The solution IR spectrum (CH₂Cl₂) shows a stretch at 1738 cm⁻¹ which shifts upon ¹³C substitution to 1698 cm⁻¹. A triplet of quintets at δ +243.66 ppm is observed (¹J_{Rh-C} = 42 Hz, ²J_{C-P} = 8 Hz) in the ¹³C{¹H} NMR spectrum. Both the energy of the CO stretch and the triplet of quintets observed in the ¹³C NMR spectrum compare favorably with known A-frames which contain a μ -CO ligand.^{18,19,21,24-28}

The reaction of $\text{Rh}_2(\mu\text{-CO})\text{Cl}_2(\text{Ph}_2\text{Ppy})_2$ with NaBH₄ in 1:3:1 mixture of THF/CH₂Cl₂/MeOH leads to formation of the borohydride complex $\text{Rh}_2(\mu\text{-CO})(\text{BH}_4)_2(\text{Ph}_2\text{Ppy})_2$, **5**, which is



(24) Cowie, M. *Inorg. Chem.* **1979**, *18*, 286-292.

(25) Cowie, M.; Southern, T. G. *Inorg. Chem.* **1982**, *21*, 246-253.

(26) Cowie, M.; Mague, J. T.; Sanger, A. R. *J. Am. Chem. Soc.* **1978**, *100*, 3628-3629.

(27) Holah, P. G.; Hughes, A. N.; Mirza, H. A.; Thompson, J. D. *Inorg. Chim. Acta* **1987**, *126*, L7-L8.

(28) Lee, C.-L.; Hunt, C. T.; Balch, A. L. *Inorg. Chem.* **1981**, *20*, 2498-2504.

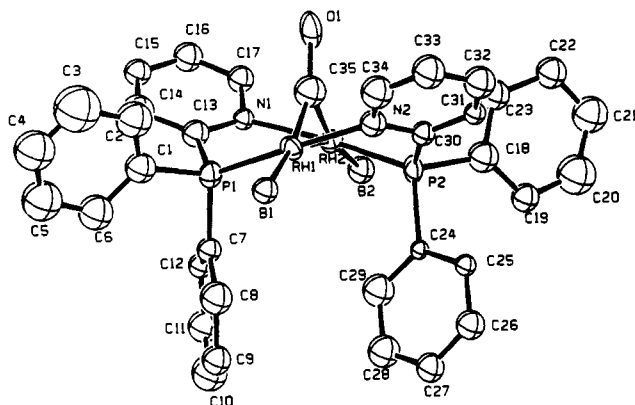


Figure 1. Perspective view of $\text{Rh}_2(\mu\text{-CO})(\text{BH}_4)_2(\text{Ph}_2\text{Ppy})_2$ (**5**), showing the skewed orientation of the P–Rh–N axes for the distorted A-frame geometry. The isotropic thermal parameter for C(35) is set to 4.0 only in this figure.

recrystallized from $\text{CH}_2\text{Cl}_2/\text{Et}_2\text{O}$. The complex is an air-stable red solid soluble in CH_2Cl_2 , CHCl_3 , benzene, toluene, and acetone. The room-temperature ^1H NMR spectrum (C_6D_6) of $\text{Rh}_2(\mu\text{-CO})(\text{BH}_4)_2(\text{Ph}_2\text{Ppy})_2$, **5**, exhibits a resonance at δ –0.09 (broad, 8 H) ppm corresponding to coordinated BH_4^- and resonances assignable to the Ph_2Ppy ligand at δ 6.22 (t, 2 H), δ 6.43 (t, 2 H), δ 6.51 (d, 2 H), and δ 9.11 (d, 2 H) for the pyridyl protons and at δ 6.9–7.8 (20 H) for overlapping phenyl protons. The one broad resonance for the BH_4^- protons indicates that these protons are undergoing rapid exchange on the NMR time scale. By ^{31}P NMR spectroscopy, a single second-order pattern is observed at δ +44.45 ppm which is slightly shifted from that of the starting complex $\text{Rh}_2(\mu\text{-CO})\text{Cl}_2(\text{Ph}_2\text{Ppy})_2$.¹⁹ The IR spectrum (KBr) shows a band at 1783 cm^{-1} indicative of a bridging CO ligand. Stretches at 2421 , 2383 cm^{-1} (strong), 1383 cm^{-1} (medium), and 1138 cm^{-1} are assigned to the coordinated BH_4^- ligands on the basis of the fact that these bands shift in the infrared spectrum of the deuterated analog $\text{Rh}_2(\mu\text{-CO})(\text{BD}_4)_2(\text{Ph}_2\text{Ppy})_2$, **5-d₈**; in the latter spectrum one of the borodeuteride bands is observed at 1727 cm^{-1} while the others are obscured by other vibrational modes of **5-d₈**.

Solid-State Structure of $\text{Rh}_2(\mu\text{-CO})(\text{BH}_4)_2(\text{Ph}_2\text{Ppy})_2$, **5.** A single-crystal X-ray diffraction study established the geometry of complex **5** as shown in the perspective drawing of Figure 1. A summary of data collection parameters, crystallographic data, and refinement information is given in Table I. The complex crystallizes in the triclinic space group $P\bar{1}$ with two independent binuclear complexes per unit cell. The structures of the two independent molecules are virtually the same with one minor difference described below. Therefore, the structural discussion focuses on the average structure except where noted. The structure of **5** is that of a distorted A-frame with the Ph_2Ppy ligands bridging the two Rh metal ions in a head to tail fashion, with each Rh center coordinated to one phosphine and one pyridyl nitrogen donor in a nearly trans orientation. The carbonyl ligand bridges the two metal centers at the apex of the A-frame, while coordinated BH_4^- groups occupy the legs of the structure. From the crystallographic data it is not possible to determine the mode of BH_4^- coordination as η^1 or η^2 unambiguously.

Complex **5** has approximate C_2 symmetry with the 2-fold axis along the C–O bond vector. The distortion from a true A-frame geometry is similar to that observed in the starting complex $\text{Rh}_2(\mu\text{-CO})\text{Cl}_2(\text{Ph}_2\text{Ppy})_2$ ¹⁹ and is consistent with the smaller bite and geometric constraint of the bridging ligand. Selected bond lengths, bond angles, and final positional parameters are given in Tables II–IV, respectively. The average Rh–Rh distance of $2.645(5)\text{ \AA}$ is similar to the Rh–Rh single bond value of $2.612(1)\text{ \AA}$ in the $\text{Rh}_2(\mu\text{-CO})\text{Cl}_2(\text{Ph}_2\text{Ppy})_2$ starting material.¹⁹ This value is slightly shorter than other Rh–Rh single bond distances as in $\text{Rh}_2(\mu\text{-SiPhH})\text{H}_2(\text{CO})_2(\text{dppm})_2$ ($2.813(1)\text{ \AA}$), $\text{Rh}_2(\mu\text{-CO})$

Table II. Intramolecular Bond Distances (\AA) for $\text{Rh}_2(\text{CO})(\text{BH}_4)_2(\text{Ph}_2\text{Ppy})_2$ (**5**)

Rh(1)–Rh(2)	2.639(5)	Rh(3)–P(3)	2.23(1)
Rh(1)–P(1)	2.19(1)	Rh(3)–N(4)	2.10(3)
Rh(1)–N(2)	2.06(4)	Rh(3)–C(70)	1.92(5)
Rh(1)–C(35)	1.64(6)	Rh(3)–B(3)	2.29(4)
Rh(2)–P(2)	2.22(1)	Rh(4)–P(4)	2.21(1)
Rh(2)–N(1)	2.17(3)	Rh(4)–N(3)	2.14(3)
Rh(2)–C(35)	1.95(6)	Rh(4)–C(70)	1.94(5)
Rh(2)–B(2)	2.23(5)	Rh(4)–B(4)	2.35(5)
Rh(3)–Rh(4)	2.650(5)	O(1)–C(35)	1.38(6)
		O(2)–C(70)	1.19(5)

Table III. Intramolecular Bond Angles (deg) for $\text{Rh}_2(\text{CO})(\text{BH}_4)_2(\text{Ph}_2\text{Ppy})_2$ (**5**)

Rh(2)–Rh(1)–P(1)	80.2(4)	P(3)–Rh(3)–N(4)	172(1)
Rh(2)–Rh(1)–N(2)	94(1)	P(3)–Rh(3)–C(70)	97(1)
Rh(2)–Rh(1)–C(35)	47(2)	P(3)–Rh(3)–B(3)	97(1)
Rh(2)–Rh(1)–B(1)	159(1)	N(4)–Rh(3)–C(70)	82(2)
P(1)–Rh(1)–N(2)	174(1)	N(4)–Rh(3)–B(3)	86(1)
P(1)–Rh(1)–C(35)	97(2)	C(70)–Rh(3)–B(3)	151(2)
N(2)–Rh(1)–C(35)	79(2)	Rh(3)–Rh(4)–P(4)	80.1(4)
C(35)–Rh(1)–B(1)	153(3)	Rh(3)–Rh(4)–N(3)	93(1)
Rh(1)–Rh(2)–P(2)	78.9(4)	Rh(3)–Rh(4)–C(70)	46(1)
Rh(1)–Rh(2)–N(1)	94.4(9)	Rh(3)–Rh(4)–B(4)	157(1)
Rh(1)–Rh(2)–C(35)	38(2)	P(4)–Rh(4)–N(3)	173(1)
Rh(1)–Rh(2)–B(2)	160(1)	P(4)–Rh(4)–C(70)	93(1)
P(2)–Rh(2)–N(1)	173(1)	P(4)–Rh(4)–B(4)	95(1)
P(2)–Rh(2)–C(35)	90(2)	N(3)–Rh(4)–C(70)	83(2)
P(2)–Rh(2)–B(2)	96(1)	N(3)–Rh(4)–B(4)	90(2)
N(1)–Rh(2)–C(35)	87(2)	C(70)–Rh(4)–B(4)	156(2)
N(1)–Rh(2)–B(2)	89(2)	Rh(1)–C(35)–Rh(2)	94(3)
C(35)–Rh(2)–B(2)	162(2)	Rh(1)–C(35)–O(1)	145(5)
Rh(4)–Rh(3)–P(3)	78.5(4)	Rh(2)–C(35)–O(1)	120(4)
Rh(4)–Rh(3)–N(4)	96(1)	Rh(3)–C(70)–Rh(4)	87(2)
Rh(4)–Rh(3)–C(70)	47(1)	Rh(3)–C(70)–O(2)	135(4)
Rh(4)–Rh(3)–B(3)	162(1)	Rh(4)–C(70)–O(2)	1138(4)

$\text{Br}_2(\text{dppm})_2$ ($2.7566(8)\text{ \AA}$), $\text{Rh}_2(\mu\text{-CF}_3\text{C}_2\text{CF}_3)\text{Cl}_2(\text{dppm})_2$ ($2.7447(9)\text{ \AA}$), and $\text{Rh}_2(\mu\text{-CO})(\text{CO})_2(\mu\text{-Cl})(\text{dppm})_2^+$ ($2.841(1)\text{ \AA}$) and provides further indication of the constrained nature of the Ph_2Ppy ligand bridge in comparison with dppm in bis(phosphine)-bridged systems.^{4,5,12,18} The head-to-tail orientation of the Ph_2Ppy ligand also introduces chirality at both metal centers.

The structural difference between the two independent molecules in the unit cell is found in the parameters of the bridging carbonyl ligand. For one of the molecules, $\mu\text{-CO}$ is symmetrically disposed between the two Rh atoms, whereas for the other the bridging carbonyl refines to a slightly asymmetric mode of coordination. The asymmetry in the latter is based solely on the final refined position of the carbonyl carbon, C(35). We attribute no significance to the refined asymmetry of $\mu\text{-CO}$ containing C(35) because its interligand contacts within the complex are less reasonable than those of C(70) which is part of the symmetric CO bridge. Thus, it appears that C(35) has refined to a false minimum, but efforts to refine the positional parameters of C(35) to a more symmetrical location have been unsuccessful. Bond distances and angles are provided for both independent molecules in the asymmetric unit, but we consider both molecules to have the same structure with the bridging carbonyl symmetrically disposed.

Mode of BH_4^- Coordination. A number of bonding modes have been identified for tetrahydridoborate complexes. The most common is bidentate or η^2 bonding of the BH_4^- ligand, but mono- and tridentate structures are also known where either one or three B–H units form bridges to the metal.^{29–34} Fluxionality in

(29) Corey, E. J.; Cooper, N. J.; Canning, W. M.; Lipscomb, W. N.; Koetzle, T. F. *Inorg. Chem.* **1982**, *21*, 192–199.

(30) Crabtree, R. H.; Pearman, A. J. *J. Organomet. Chem.* **1978**, *157*, 345–352.

(31) Empsall, H. D.; Mentzer, E.; Shaw, B. L. *J. Chem. Soc., Chem. Commun.* **1975**, 861–862.

(32) Letts, J. B.; Mazanec, T. J.; Meek, D. W. *J. Am. Chem. Soc.* **1982**, *104*, 3898–3905.

Table IV. Positional Parameters and B_{eq} Values for $\text{Rh}_2(\text{CO})(\text{BH}_4)_2(\text{Ph}_2\text{Ppy})_2$ (**5**)

atom	x	y	z	B_{eq} (\AA^2)	atom	x	y	z	B_{eq} (\AA^2)
Rh(1)	0.7953(4)	0.2462(2)	0.9001(2)	2.2(3)	C(31)	0.709(4)	0.095(3)	0.765(2)	2(1)
Rh(2)	0.9546(3)	0.2811(2)	0.8124(2)	2.1(3)	C(32)	0.674(4)	0.025(3)	0.791(2)	4(1)
Rh(3)	0.4818(4)	0.2175(2)	0.2780(2)	2.3(3)	C(33)	0.667(4)	0.022(3)	0.850(2)	5(1)
Rh(4)	0.6465(4)	0.1957(2)	0.3586(2)	2.5(3)	C(34)	0.701(4)	0.086(3)	0.880(2)	4(1)
P(1)	0.869(1)	0.3458(8)	0.9409(5)	3(1)	C(35)	0.934(6)	0.192(4)	0.869(3)	8(2)
P(2)	0.801(1)	0.2481(8)	0.7650(5)	3(1)	C(36)	0.622(4)	0.058(3)	0.175(2)	2(1)
P(3)	0.614(1)	0.0934(8)	0.2497(5)	3(1)	C(37)	0.596(5)	0.122(3)	0.133(2)	5(1)
P(4)	0.467(1)	0.2579(8)	0.4122(6)	3(1)	C(38)	0.605(5)	0.096(4)	0.075(2)	6(2)
O(1)	1.031(3)	0.120(2)	0.872(1)	4(2)	C(39)	0.632(5)	0.010(4)	0.057(2)	6(1)
O(2)	0.657(3)	0.333(2)	0.273(1)	5(3)	C(40)	0.648(5)	-0.054(3)	0.100(2)	5(1)
N(1)	1.086(3)	0.318(2)	0.868(1)	1.8(8)	C(41)	0.644(4)	-0.030(3)	0.155(2)	2(1)
N(2)	0.736(3)	0.155(2)	0.854(2)	2.8(9)	C(42)	0.603(4)	0.002(3)	0.296(2)	2(1)
N(3)	0.806(4)	0.135(2)	0.299(2)	3(1)	C(43)	0.485(4)	0.003(3)	0.334(2)	2(1)
N(4)	0.359(3)	0.328(2)	0.316(1)	2.2(8)	C(44)	0.468(4)	-0.068(3)	0.362(2)	2(1)
C(1)	0.857(4)	0.351(3)	1.018(2)	4(1)	C(45)	0.565(4)	-0.140(3)	0.359(2)	3(1)
C(2)	0.881(5)	0.277(3)	1.045(2)	5(1)	C(46)	0.677(5)	-0.140(3)	0.329(2)	4(1)
C(3)	0.863(6)	0.269(4)	1.112(3)	9(2)	C(47)	0.700(5)	-0.076(3)	0.292(2)	5(1)
C(4)	0.827(5)	0.342(4)	1.141(2)	7(2)	C(48)	0.781(4)	0.097(3)	0.251(2)	2(1)
C(5)	0.806(5)	0.420(4)	1.111(3)	6(2)	C(49)	0.885(5)	0.065(3)	0.206(2)	5(1)
C(6)	0.820(5)	0.429(3)	1.048(2)	5(1)	C(50)	1.005(5)	0.077(3)	0.218(2)	5(1)
C(7)	0.804(4)	0.453(3)	0.920(2)	2(1)	C(51)	1.037(5)	0.114(3)	0.263(2)	5(1)
C(8)	0.676(5)	0.487(3)	0.928(2)	4(1)	C(52)	0.931(6)	0.147(4)	0.304(3)	8(2)
C(9)	0.610(4)	0.571(3)	0.913(2)	3(1)	C(53)	0.362(4)	0.187(3)	0.438(2)	2(1)
C(10)	0.688(5)	0.624(3)	0.887(2)	5(1)	C(54)	0.251(5)	0.185(3)	0.414(2)	4(1)
C(11)	0.814(5)	0.592(3)	0.878(2)	4(1)	C(55)	0.173(6)	0.118(4)	0.437(3)	8(2)
C(12)	0.874(4)	0.509(3)	0.897(2)	2(1)	C(56)	0.219(5)	0.064(3)	0.476(2)	4(1)
C(13)	1.037(4)	0.340(3)	0.924(2)	3(1)	C(57)	0.324(5)	0.067(3)	0.498(2)	3(1)
C(14)	1.129(5)	0.352(3)	0.964(2)	4(1)	C(58)	0.393(4)	0.123(3)	0.481(2)	2(1)
C(15)	1.265(4)	0.335(3)	0.942(2)	3(1)	C(59)	0.483(5)	0.315(3)	0.483(2)	4(1)
C(16)	1.308(4)	0.308(3)	0.887(2)	3(1)	C(60)	0.584(6)	0.359(4)	0.472(3)	7(2)
C(17)	1.221(4)	0.298(3)	0.850(2)	3(1)	C(61)	0.607(5)	0.403(3)	0.524(3)	6(2)
C(18)	0.838(4)	0.217(3)	0.689(2)	4(1)	C(62)	0.512(6)	0.407(3)	0.572(2)	6(2)
C(19)	0.783(4)	0.255(3)	0.642(2)	3(1)	C(63)	0.413(5)	0.370(4)	0.575(2)	6(2)
C(20)	0.831(5)	0.216(4)	0.588(2)	6(1)	C(64)	0.386(5)	0.319(3)	0.527(2)	5(1)
C(21)	0.934(5)	0.144(3)	0.576(2)	5(1)	C(65)	0.359(4)	0.344(3)	0.373(2)	3(1)
C(22)	0.992(4)	0.104(3)	0.620(2)	4(1)	C(66)	0.282(4)	0.418(3)	0.403(2)	3(1)
C(23)	0.951(4)	0.146(3)	0.677(2)	4(1)	C(67)	0.213(4)	0.481(3)	0.368(2)	3(1)
C(24)	0.643(4)	0.327(3)	0.764(2)	1(1)	C(68)	0.215(4)	0.469(3)	0.308(2)	5(1)
C(25)	0.543(4)	0.301(3)	0.742(2)	2(1)	C(69)	0.288(5)	0.389(3)	0.283(2)	4(1)
C(26)	0.430(4)	0.362(3)	0.740(2)	3(1)	C(70)	0.612(4)	0.277(3)	0.295(2)	2(1)
C(27)	0.419(4)	0.446(3)	0.760(2)	3(1)	B(1)	0.610(5)	0.261(3)	0.963(2)	3(1)
C(28)	0.517(5)	0.470(3)	0.783(2)	4(1)	B(2)	1.036(5)	0.353(3)	0.739(2)	3(1)
C(29)	0.634(4)	0.408(3)	0.785(2)	4(1)	B(3)	0.314(4)	0.206(3)	0.226(2)	0(1)
C(30)	0.738(4)	0.158(3)	0.796(2)	2(1)	B(4)	0.753(5)	0.130(3)	0.438(2)	3(1)

BH_4^- -ligated systems is the rule rather than the exception, and very low barriers for terminal and bridging B-H exchange often make assignment of bonding difficult, even with low-temperature NMR spectroscopy (200 K). For complex **2**, the slow-exchange limit is not reached at -95°C , at which point solubility limitations become a factor. For complex **5**, low-temperature ^1H NMR spectra obtained at 198 K show three featureless resonances at $\delta -3.25$ (1 H), -3.77 (2 H), and $+0.05$ (1 H) ppm in place of the single resonance at $\delta -0.09$ ppm at 298 K. The chemical shifts, however, are atypical of bridging Rh-H-B and terminal B-H protons in comparison with other known ruthenium and rhodium systems, obviating a definitive assignment of borohydride bonding mode.

According to Marks, IR spectroscopy is most useful for determining the binding mode of coordinated BH_4^- ligands due to the fast time scale of the technique, the medium-to-strong intensity of B-H stretches, and the region in which they appear.³³ On the basis of a comparison of IR spectra of borohydride and borodeuteride complexes, complex **2** exhibits BH_4^- bands at 2422, 2384, 1364, and 1145 cm^{-1} in CH_2Cl_2 solution, while **5** shows borohydride modes at 2397, 2358, 1371, and 1135 cm^{-1} . The two higher energy stretches for each complex are consistent with either a monodentate or bidentate bonding mode, while the lowest energy band for each, corresponding to a deformation, is

compatible with all four possible modes of borohydride coordination. It is the presence of the 1364- and 1371- cm^{-1} bands in **2** and **5**, respectively, however, that makes possible the assignment of BH_4^- coordination in these complexes as bidentate since bands in this range are only expected for doubly bridging or η^2 BH_4^- ligands. This assignment of η^2 coordination of the BH_4^- ligands in **2** and **5** compares favorably with other systems where bidentate bonding of BH_4^- ligand is the most common mode of coordination.^{29,31-34} The structures of **2** and **5** are thus similar A-frame arrangements with bridging carbonyls and borohydride ligands as the "legs" of the structure with η^2 coordination.

Formation of the Tetrahydride Complex $\text{Rh}_2(\mu\text{-H})_2\text{H}_2(\text{CO})(\text{dppm})_2$, **3.** When the borohydride reduction of $\text{Rh}_2\text{Cl}_2(\mu\text{-CO})(\text{dppm})_2$ is carried out in THF/MeOH, or when complex **2** is dissolved in a 3:1 (v/v) mixture of THF/MeOH for 30 min, an orange solution of a new species is formed. Upon addition of cold olefin-free hexanes, an orange precipitate forms which is filtered out in air, yielding an air-stable solid of complex **3**. Under vacuum or after 1 h under N_2 , complex **3** turns dark green but reverts to the orange color when placed under a stream of H_2 . Complex **3** is soluble in THF, C_6D_6 , Et_2O , and toluene and insoluble in hexanes and acetone. The room-temperature ^1H NMR spectrum (THF- d_6) of either the orange or green forms of complex **3** exhibits two broad hydride resonances at $\delta -9.24$ and -10.45 ppm as shown in Figure 2a, while the $\text{dppm}-\text{CH}_2$ -protons appear as a broad singlet at $\delta +4.04$ ppm with unresolved phosphorus couplings. When a THF- d_6 solution of complex **3** is

(33) Marks, T. J.; Kolb, J. R. *Chem. Rev.* **1977**, *77*, 263-293.

(34) Wink, D. J.; Cooper, N. J. *J. Chem. Soc., Dalton Trans.* **1984**, 1257-1259.

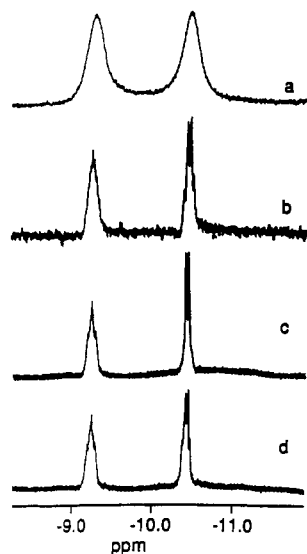


Figure 2. Hydride region in the ^1H NMR spectrum of complex **3**: (a) room temperature, (b) 233 K, (c) P_1 (δ 47.4 ppm) decoupled, and (d) P_2 (δ 37.8 ppm) decoupled.

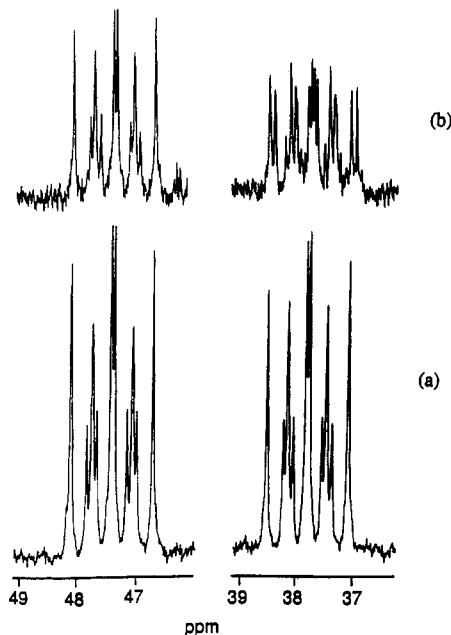


Figure 3. (a) $^{31}\text{P}\{^1\text{H}\}$ NMR spectrum of complex **3**. (b) $^{31}\text{P}\{^1\text{H}\}$ NMR spectrum of complex **3** with ^{13}C O. Only the δ 37.8 ppm resonance exhibits ^{13}C coupling.

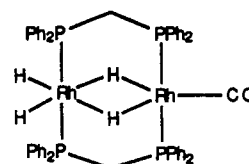
placed under 1–3 atm of H_2 , the two hydride resonances and the $\text{dppm}-\text{CH}_2$ -resonance integrate as 2:2:4 protons. In the absence of excess H_2 in solution, the intensities of the hydride resonances diminish slightly, while all other resonances remain unchanged in the spectrum. When a sample of **3** is cooled to -40°C , the resonance at δ -10.45 (q , $J_{\text{Rh-H, P-H}} = 17\text{Hz}$) becomes structured while the other resonance at δ -9.24 , ($J_{\text{Rh-H, P-H}}$, unresolved) remains broad as shown in Figure 2b. When a sample of complex **3** is heated to 40°C in an NMR tube, the two hydride signals coalesce whereas all other resonances in the ^1H and ^{31}P NMR spectra remain unchanged. The 40°C coalescence of hydride resonances shows that exchange is occurring between the two hydride sites.

The $^{31}\text{P}\{^1\text{H}\}$ NMR spectrum of **3** exhibits two resonances which appear as identical second-order patterns at δ $+47.4$ and δ $+37.8$ ppm in $\text{THF}-d_8$ as shown in Figure 3a. The $^{31}\text{P}\{^1\text{H}\}$ NMR spectrum of the ^{13}C O-labeled complex exhibits an additional coupling to only one of the two resonances (the one at δ $+37.8$ ppm), as shown in Figure 3b. The fully coupled ^{31}P NMR

spectrum of **3** reveals that the δ 47.4 ppm resonance is more noticeably broadened relative than the one at δ 37.8 ppm. The IR spectrum exhibits a band at 1965 cm^{-1} (KBr) (1932 cm^{-1} in THF/MeOH) which shifts upon ^{13}C O substitution to 1878 cm^{-1} (KBr). The hydride stretches were not observed by IR spectroscopy.

Selective heteronuclear $^1\text{H}\{^{31}\text{P}\}$ NMR decoupling experiments were performed to analyze the phosphorus–hydride couplings more fully in order to make a definitive structural assignment for complex **3**. When the phosphorus resonance at δ $+47.4$ ppm (P_1) is decoupled, the hydride resonance at δ -10.45 ppm simplifies to a doublet, while that at δ -9.24 becomes a broad pseudotriplet, whereas when the resonance at δ $+37.8$ ppm (P_2) is selectively decoupled, the hydride resonance at δ -10.45 ppm remains unchanged while that at δ -9.24 ppm becomes the same pseudotriplet as before. These changes are shown in Figure 2c,d.

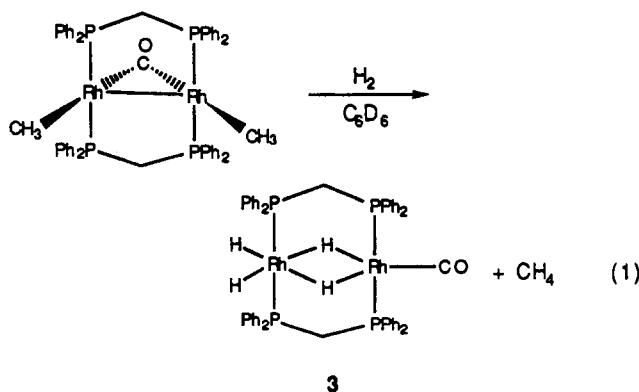
On the basis of the spectroscopic evidence outlined above showing two inequivalent hydrides, two inequivalent ^{31}P nuclei, and a terminal CO, which upon ^{13}C labeling shows coupling to only one of the two ^{31}P resonances, we formulate the orange/green solid as the binuclear tetrahydride complex $\text{Rh}_2\text{H}_2(\mu\text{-H})_2(\text{CO})(\text{dppm})_2$, **3**, having the structure shown as follows:



3

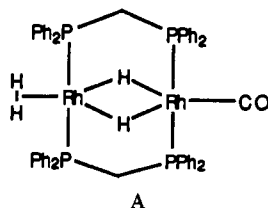
One of the Rh atoms is in an octahedral environment, ligated axially by the dppm phosphines and equatorially by four hydrides, while the other Rh atom has a five-coordinate trigonal bipyramidal geometry containing two bridging hydrides, a terminal CO in its equatorial plane, and axially coordinated dppm phosphines.

Complex **3** is also observed to form as the only metal-containing product in the reaction of a C_6D_6 solution of $\text{Rh}_2(\mu\text{-CO})(\text{CH}_3)_2(\text{dppm})_2$, which has been characterized previously to have a $\mu\text{-CO}$ A-frame structure,²¹ with 1 atm of H_2 . Methane is also generated in this reaction shown as eq 1, as evidenced by the appearance of a singlet at δ 0.2 ppm in the ^1H NMR spectrum.



3

The reversible loss of H_2 from complex **3** in the solid state and the identical second-order phosphorus patterns for both sets of phosphine donors consistent with the same $J_{\text{Rh-P}}$ and oxidation state for the two Rh centers suggested the possibility that **3** is actually a dihydride dihydrogen complex shown as A rather than a classical tetrahydride system.³⁵ To assess this formulation of **3**, T_1 measurements and an analysis of the isotopomer formed under HD were performed. Through the inversion recovery

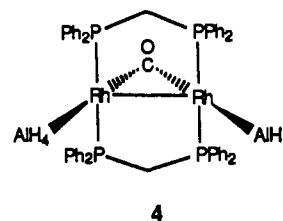


method at various temperatures, values of T_1 were determined which gave a T_1 minimum value of 560 and 651 ms for terminal and bridging hydrides, respectively, at 243 K (400 MHz).³⁶⁻⁴⁵ Both values are well outside of the range expected for a molecular hydrogen complex and are consistent with a classical tetrahydride formulation. Further support for this conclusion comes from the absence of any HD coupling when complex 3 is dissolved in C_6D_6 and placed under 1 atm of HD. Dihydrogen complexes exhibit large couplings (10–35 Hz) in their HD isotopomers.³⁶⁻⁴⁵

The tetrahydride complex 3 is one of very few rhodium polyhydride systems that have been reported. Other systems include the hexahydride species $Rh_2(H)_6(dcpm)_2$ (dcpm = 1,1-bis(dicyclohexylphosphino)methane) described by Fryzuk⁴⁶ and the tetrahydride complex $Rh_2H_4\{P[N(CH_3)_2]_3\}_4$ reported by Muetterties.⁴⁷

Reduction with $LiAlH_4$. The $LiAlH_4$ reduction of $Rh_2Cl_2(\mu-CO)(dppm)_2$ in THF- d_8 yields an extremely air-sensitive orange solution which decomposes upon workup even at low temperatures as observed by 1H and $^{31}P\{^1H\}$ NMR spectroscopies. Attempts to isolate the complex in this solution, which is generated along with a small amount of free dppm, have proven unsuccessful to date. When MeOH or EtOH is added to the solution, clean conversion to complex 3 is observed. The 1H NMR (THF- d_8) spectrum for the reactive complex denoted as 4 exhibits two sets of inequivalent dppm methylene protons at δ 3.00 ppm (d, 2 H) and 3.85 ppm (m, 2 H), and resonances at δ -5.10 (d, 2 H), -6.90 (unresolved, 2 H), and 2.80 ppm corresponding to AlH_4^- protons. The δ -5.10 and -6.90 ppm resonances are due to bridging Al-H protons, while the resonance at δ 2.80 arises from the terminal Al-H protons. Solvent and dppm $-CH_2-$ resonances overlap with the δ 2.80 ppm resonance, the intensity of which varies with the amount of excess $LiAlH_4$ present, making integration of this peak unreliable. Two sets of phenyl resonances are also observed between δ 6.88–7.94 ppm. The ^{31}P NMR spectrum exhibits a single symmetric second-order pattern at δ 52.8 ppm ($J_{Rh-P} = 137.6$ Hz), while the IR spectrum exhibits a CO stretch at 1693 cm^{-1} assignable to a bridging CO ligand. The low value of ν_{CO} may be due to strong donation of the AlH_4^- ligands into the $\mu-CO$ ligand. A triplet of quintets at δ 271.6 ppm ($J_{Rh-C} = 32.7$ Hz, $J_{C-P} = 9$ Hz) is also observed in the $^{13}C\{^1H\}$ NMR spectrum, consistent with a bridging CO ligand coupled to two equivalent Rh nuclei as well as four equivalent phosphorus atoms. A similar

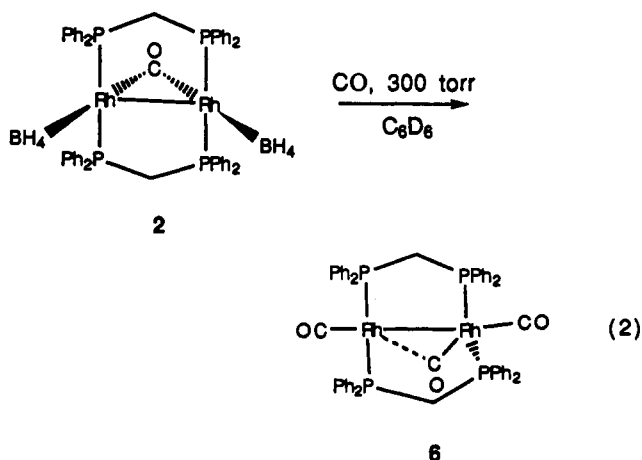
pattern was observed for the borohydride complex 2. When excess $NaBH_4$ was added to a THF- d_8 solution of complex 4, partial conversion to complex 2 was observed via simple exchange of AlH_4^- with BH_4^- . On the basis of these results, we propose that complex 4 has an A-frame geometry with CO in the bridgehead position and two AlH_4^- ligands in the legs of the structure, analogous to the borohydride complexes 2 and 5.



Reactions with D_2 . The reactions of complexes 2 and 5 with D_2 were examined by 1H NMR spectroscopy to investigate H/D exchange into the borohydride ligands. For complex 2 under 0.5 atm D_2 , a 1:1:1 triplet at δ +4.45 ppm characteristic of free HD was observed after 15 min at room temperature along with a 25% decrease in the intensity in the BH_4^- resonance at δ -1.49 ppm. For $Rh_2(\mu-CO)(BH_4)_2(Ph_2Ppy)_2$ (5), exchange was substantially slower with only a 6% decrease in the borohydride intensity noted after 17 h at room temperature under 1 atm of D_2 . H/D exchange with the tetrahydridoaluminate complex 4 was also found to be relatively slow. When a THF- d_8 solution 4 was placed under 1 atm of D_2 , a weak 1:1:1 triplet at δ 4.53 ppm characteristic of free HD was seen after 1.5 h at ambient temperature. However, accurate estimation of the extent of H/D exchange was not possible because of exchange between complexed AlH_4^- and excess $LiAlH_4$ in the sample.

When the tetrahydride complex 3 is placed under 1 atm D_2 , the intensities of both hydride resonances diminish simultaneously. At -30 °C, both H_2 and HD appear to be liberated simultaneously in the exchange reaction, as seen by a singlet at δ 4.42 ppm and a 1:1:1 triplet at δ +4.45 ppm, respectively, in the 1H NMR spectrum. As deuterium incorporation proceeds, the ^{31}P NMR spectrum shows significant broadening in the δ 47.4 ppm resonance, while the other resonance at δ 37.8 ppm broadens only slightly. The relative broadening of ^{31}P resonances is consistent with the unsymmetrical structure of 3. Deuterium exchange was also observed when MeOD was added to a THF- d_8 solution of complex 3.

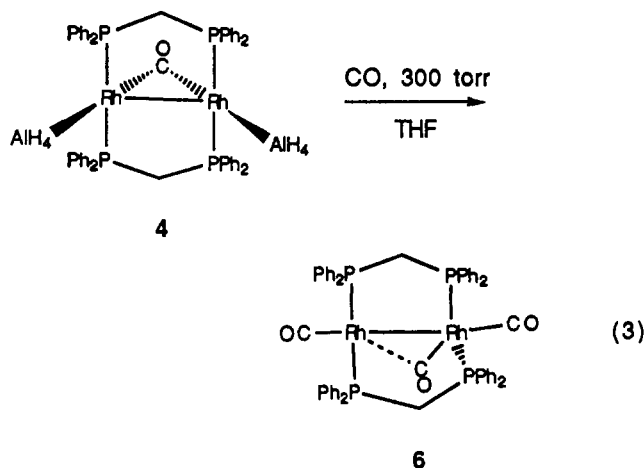
Reactions with CO. The borohydride complex 2 with reacts with as little as 300 Torr of CO in an NMR tube to afford the known tricarbonyl complex $Rh_2(CO)_3(dppm)_2$, 6, quantitatively (eq 2), as evidenced by resonances at δ 4.43 and 7.15–7.81 ppm



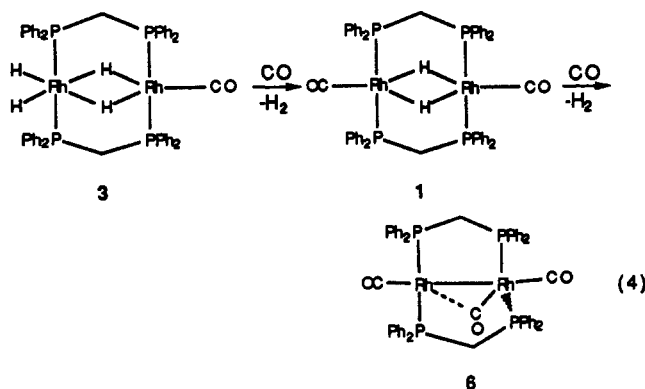
in the 1H NMR spectrum and at 19.19 ppm in the $^{31}P\{^1H\}$ NMR spectrum characteristic of an authentic sample of 6. The

- (36) Ammann, C.; Isaia, F.; Pregosin, P. S. *Magn. Reson. Chem.* **1988**, *26*, 236–238.
- (37) Chinn, M. S.; Heinekey, D. M. *J. Am. Chem. Soc.* **1987**, *109*, 5865–5867.
- (38) Cotton, F. A.; Luck, R. L.; Root, D. R.; Walton, R. A. *Inorg. Chem.* **1990**, *29*, 43–47.
- (39) Bautista, M.; Earl, K. A.; Morris, R. H.; Sella, A. *J. Am. Chem. Soc.* **1987**, *109*, 3780–3782.
- (40) Bautista, M. T.; Earl, K. A.; Maltby, P. A.; Morris, R. H.; Schweitzer, C. T.; Sella, A. *J. Am. Chem. Soc.* **1988**, *110*, 7031–7036.
- (41) Kubas, G. J.; Ryan, R. R.; Swanson, B. I.; Vergamini, P. J.; Wasserman, H. J. *J. Am. Chem. Soc.* **1984**, *106*, 451–452.
- (42) Kubas, G. J.; Unkefer, C. J.; Swanson, B. I.; Fukushima, E. *J. Am. Chem. Soc.* **1986**, *108*, 7000–7009.
- (43) Kubas, G. J.; Ryan, R. R.; Wroblewski, D. A. *J. Am. Chem. Soc.* **1986**, *108*, 1339–1341.
- (44) Kubas, G. *J. Acc. Chem. Res.* **1988**, *21*, 120–128.
- (45) Hamilton, D. G.; Crabtree, R. H. *J. Am. Chem. Soc.* **1988**, *110*, 4126–4133.
- (46) Fryzuk, M. *J. Organomet. Chem.* **1992**, *440*, in press.
- (47) Meier, E. B.; Burch, R. R.; Muetterties, E. L.; Day, V. W. *J. Am. Chem. Soc.* **1982**, *104*, 2663–2664.

tetrahydridoaluminate species **4** reacts similarly. When a THF- d_8 solution of complex **4** is placed under 400 Torr of CO in an NMR tube, the formation of complex **6** occurs within 15 min at room temperature (eq 3). Somewhat unexpectedly, the Ph_2Ppy -bridged borohydride complex **5** was found to be unreactive with CO.



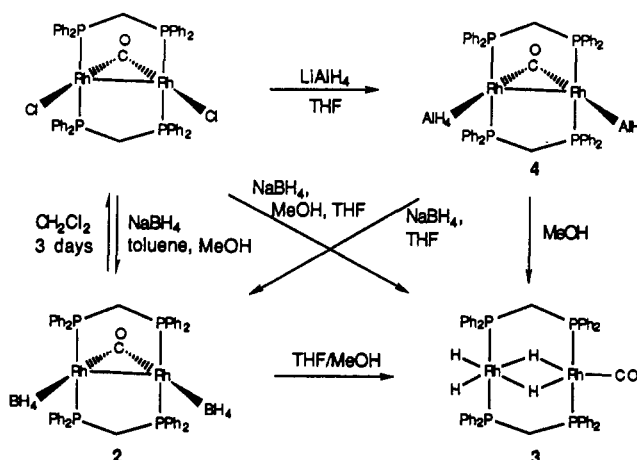
The tetrahydride complex **3** reacts rapidly with CO at room temperature to form the tricarbonyl species $\text{Rh}_2(\text{CO})_3(\text{dppm})_2$, **6**. When the reaction is followed at -30°C by ^1H and $^{31}\text{P}\{^1\text{H}\}$ NMR spectroscopies, sequential formation of the dihydride complex **1** and the tricarbonyl species **6** is observed along with the liberation of H_2 as shown in eq 4.



Catalytic Olefin Hydrogenations. The tetrahydride complex **3** and the borohydride complexes **2** and **5** exhibit some activity in the catalytic hydrogenation of olefins. Complex **3** catalyzes hydrogenation of styrene and acrylonitrile, and turnovers for each of these substrates were estimated by NMR spectroscopy as follows. Complex **3** was dissolved in C_6D_6 and its ^1H NMR spectrum integrated against an internal standard such as THF. Use of a standard is required since **3** is not observed after the addition of olefin. The sample was frozen, and a large excess of olefin was injected into the NMR tube and placed under 3 atm of H_2 . Subsequent ^1H NMR spectra were recorded at hourly intervals, and the amount of hydrogenated product was then integrated relative to the standard. By this procedure, it was found that complex **3** catalyzes styrene at the rate of 95 turnovers/h and acrylonitrile at the rate of 120 turnovers/h. During the course of the reactions, resonances from an uncharacterized metal complex were observed and this species persisted in solution even after all olefin was hydrogenated.

The tetrahydridoborate complexes **2** and **5** also catalyze olefin hydrogenation. When **2** is dissolved in CD_2Cl_2 and the solution is placed under 150 Torr of ethylene in the absence of H_2 , a singlet at δ 0.8 ppm corresponding to free ethane is observed in the ^1H NMR spectrum along with slight catalyst decomposition

Scheme I



within 10 min. After 3 h at room temperature, about 30% of **2** still remains, indicating, at least qualitatively, that the rate of hydrogenation is relatively slow in the absence of H_2 . However, when the reaction between **2** and either ethylene, styrene, or acrylonitrile is run under 3 atm of H_2 at room temperature, catalytic hydrogenation is noted at the rate of approximately 10 turnovers/h. During hydrogenation, significant decomposition of the catalyst is noted within 3 h, and after 12 h the catalyst has decomposed completely.

In the presence of 600 Torr of H_2 , complex **5** catalyzes hydrogenation of *tert*-butylethylene slowly, yielding 2.3 turnovers over 48 h at room temperature. The reaction was monitored by following the formation of 2,2-dimethylbutane via ^1H NMR spectroscopy. The analogous reaction of **5** with ethylene is much faster. Five minutes after 600 Torr of H_2 is placed over the catalyst-olefin mixture, the formation of at least 1 equiv of ethane relative to catalyst concentration is observed in solution by ^1H NMR spectroscopy.

Conclusions

Scheme I summarizes the hydride reduction of the starting material $\text{Rh}_2\text{Cl}_2(\mu\text{-CO})(\text{dppm})_2$ reported in the present work. The tetrahydridoborate and tetraaluminumohydrate A-frame complexes $\text{Rh}_2(\text{BH}_4)_2(\mu\text{-CO})(\text{dppm})_2$, **2**, and $\text{Rh}_2(\text{AlH}_4)_2(\mu\text{-CO})(\text{dppm})_2$, **4**, form by metathetical substitution of the tetrahydrido anion for Cl^- , and both complexes react further to form the rhodium tetrahydride complex $\text{Rh}_2(\text{CO})(\mu\text{-H})_2(\text{H})_2(\text{dppm})_2$, **3**. The tetrahydride complex undergoes facile H_2 loss and readdition in the solid state, but T_1 measurements show that **3** is a classical hydride complex. The Ph_2Ppy -bridged borohydride complex $\text{Rh}_2(\mu\text{-CO})(\text{BH}_4)_2(\text{Ph}_2\text{Ppy})_2$, **5**, forms by simple metathetical reaction between NaBH_4 and the corresponding chloro complex, but it does not react further to generate a polyhydride species. Complexes **2**, **3**, and **5** all show activity as olefin hydrogenation catalysts.

Acknowledgment. We wish to thank the National Science Foundation (Grant CHE 89-09060) for the financial support of this work, Johnson Matthey Co., Inc., for a generous loan of rhodium trichloride, and Dr. Kurt Kramarz for helpful suggestions.

Supplementary Material Available: Complete listing of crystallographic details and bond lengths and bond angles for **5** (10 pages). Ordering information is given on any current masthead page.